

## General need for 3D in the MDCT Era

William P. Dillon, M.D.  
Elizabeth Guillaumin Professor of Radiology,  
Neurology and Neurosurgery  
Chief, Section of Neuroradiology

Richard S. Breiman, M.D.  
Associate Clinical Professor of Radiology  
Abdominal Imaging and Ultrasound Sections  
Department of Radiology

Max Wintermark, M.D., Assistant Professor  
of Radiology  
Department of Radiology,  
Neuroradiology Section

University of California, San Francisco  
505 Parnassus Ave., Box 0628  
San Francisco, CA 94143

Fergus Coakley M.D., Chief,  
Abdominal Imaging,

### Introduction *Fergus Coakley, M.D.*

The emergence of four-row multidetector CT (MDCT) in 1998 was a major technological breakthrough that dramatically changed the practice of CT. The temporal resolution of MDCT is now comparable to MRI, the spatial resolution remains superior to MRI, and the extent of coverage exceeds MRI. MDCT may appear to be simply an incremental improvement in spiral CT technology. This view of MDCT is incomplete, since the unprecedented capability to rapidly acquire numerous thin sections in multiple phases of enhancement provides great challenges for image handling and storage, as well as great opportunities for three-dimensional post-processing and display. Multiphase imaging can now be performed routinely and with near isotropic resolution (isotropic resolution refers to equal resolution in the x, y, and z axes, so that the voxels are cubic in shape), allowing generation of exquisitely detailed three-dimensional volumetric reconstructions. Three-dimensional data sets, narrow collimation, and multiphase imaging provide improved lesion detection, multiplanar capability, and the ability to perform high-quality CT angiography.

With this evolving technology comes significant new challenges, particularly with respect to managing the vast quantity of image data that is generated. These remain as unsolved problems that will require the development of innovative image processing and viewing strategies. The traditional paradigm of reviewing tomographic slices may well be replaced by a primarily volumetric approach. It is possible that MDCT will become the key factor in promoting wide dissemination of PACS technology and three-dimensional softcopy image interpretation. The rapidity with which body cavities can be imaged with MDCT also requires new thinking with respect to the rate of intravenous contrast administration, contrast injection duration, contrast bolus volume, and scan delays. With scanning times as short as 10 seconds, smaller contrast volumes injected at a faster rate may be more appropriate. While narrow collimation may seem intuitively advantageous, it increases image noise and may reduce the geometric efficiency of the detectors. Finally, the radiation dose is increased with MDCT (although some factors can be adjusted to limit this dose increase), which is compounded by

multiphase imaging. Careful attention must be paid to technical parameters during scanning, with tailoring of the dose and imaging protocol to the clinical question. Use of commercially available dose-modifying software may help.

**Case 1: CT- angiography in a Patient with an External Carotid-internal Carotid (EC-IC) Artery Bypass**

*Max Wintermark, M.D., William P. Dillon, M.D.*

**History:**

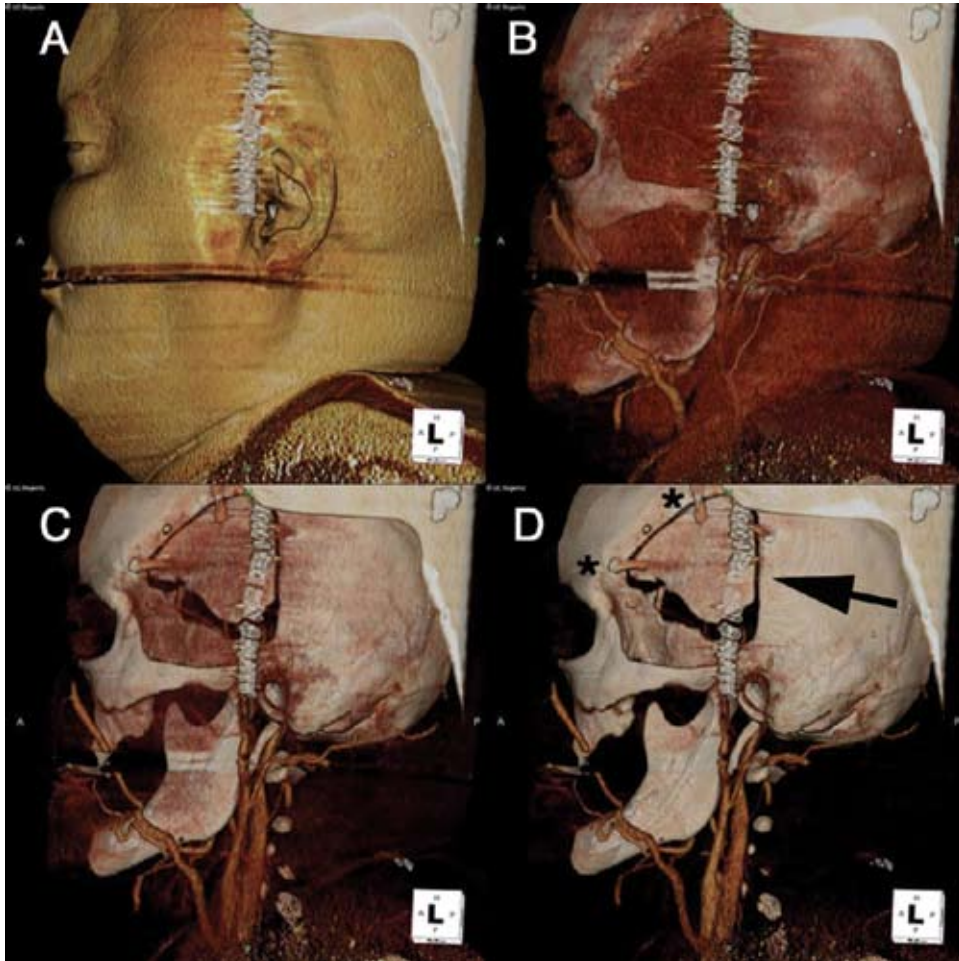
The patient is a male aged 54 with an occluded left internal carotid artery immediately superior to the carotid bifurcation. He was presented with critically low brain perfusion in the corresponding left hemisphere. He underwent an external carotid-internal carotid (EC-IC) artery bypass. CT-angiography of the cervical and intracranial vessels was requested to evaluate bypass patency.

**Protocol Description:**

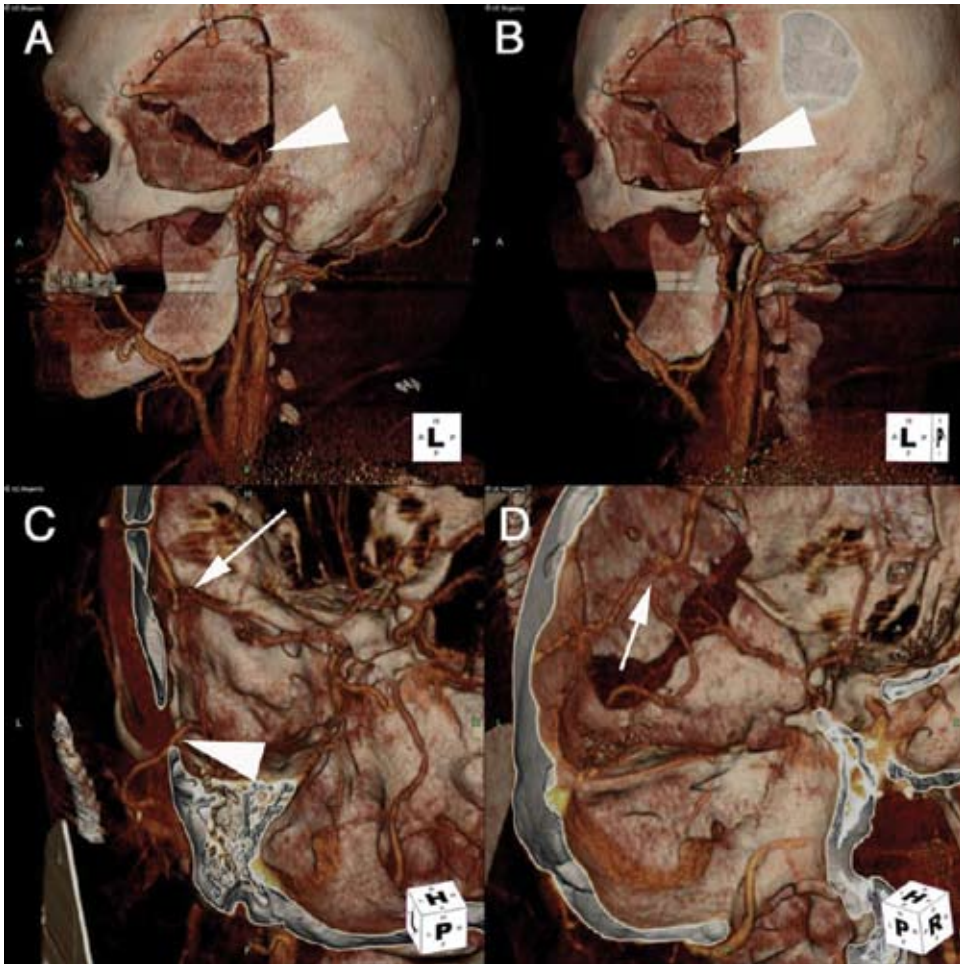
Scan Information	Type of Scanner	Lightspeed 16
	Scan Region	Head and Neck
	Scan Length	40 cm
	Scan Direction	Caudocranial
	Detector Configuration	16 x 1.25
	Pitch	1.375:1
	Tube Voltage	120 kVp
	Tube Current	240 mA
	Rotation Time	0.5 sec
	Total Acquisition Time	8 sec
	Field of View	22 cm
Reconstruction Information	Reconstruction Algorithm	Standard
	Slice Thickness	1.25
	Reconstruction Interval	1
	Total Number of Images	400
Contrast Information	Contrast	Omnipaque
	Concentration	300 mg/mL
	Volume	70 mL
	Injection Rate	4 mL/sec
	Timing Method	Bolus Test

**Results:**

3D post-processing using the Aquarius Workstation (from TeraRecon, Inc.) permits a virtual dissection of the patient, starting from the skin (A), going through the soft tissues and muscles (B and C), down to the skull (D). The craniotomy site (black arrow) is very well visualized, as are the metallic clips (stars) used to close it.



The 3D reconstructions demonstrate the left superficial temporal artery as it enters the craniotomy site (arrowheads) and connects to the branches of the left middle cerebral artery (white arrows), confirming the patency of the bypass.



### Discussion:

Using the Aquarius Workstation, 3D reconstructions from CT-angiography demonstrate the patency of the EC-IC bypass, obviating the need to perform a conventional angiogram. Timing of the CT-angiography acquisition with the contrast bolus arrival is critical in order to obtain optimal 3D reconstructions. Bolus timing for CTA is obtained either using tracking bolus software or a test bolus method. We prefer the test bolus method, as the venous enhancement is minimized so that the precise delineation of adjacent arterial structures is enhanced.

### References:

- Sameshima T, Futami S, Morita Y, Yokogami K, Miyahara S, Sameshima Y, Goya T, Wakisaka S. Clinical usefulness of and problems with three-dimensional CT angiography for the evaluation of arteriosclerotic stenosis of the carotid artery: comparison with conventional angiography, MRA, and ultrasound sonography. *Surg Neurol* 1999;51(3):301-308.
- Takamura Y, Tanooka A, Morimoto S. Usefulness of three-dimensional CT angiography (3D-CTA) with a single bolus injection of contrast material for the examination of intracranial and cervical arteries in cerebrovascular disease screening. *No Shinkei Geka* 2001;29(5):401-406.

## Case 2: CT-angiography in a Patient with Subarachnoid Hemorrhage

*Max Wintermark, M.D., William P. Dillon, M.D.*

### History:

The patient, a female aged 66, was admitted for thunderclap headaches. A non-contrast CT demonstrated a subarachnoid hemorrhage. Immediately after the CT, the patient underwent a CT-angiogram of her intracranial arteries.

### Protocol Description:

Scan Information	Type of Scanner	Lightspeed 16
	Scan Region	Skull
	Scan Length	15 cm
	Scan Direction	Caudocranial
	Detector Configuration	16 x 0.625
	Pitch	1.375:1
	Tube Voltage	120 kVp
	Tube Current	280 mA
	Rotation Time	0.5 sec
	Total Acquisition Time	6 sec
	Field of View	18 cm
Reconstruction Information	Reconstruction Algorithm	Standard
	Slice Thickness	0.625
	Reconstruction Interval	0.5
	Total Number of Images	300
Contrast Information	Contrast	Omnipaque
	Concentration	300 mg/mL
	Volume	70 mL
	Injection Rate	4 mL/sec
	Timing Method	Bolus Test

### Results:

The 3D reformations obtained from the CT-angiogram data display four aneurysms: 1) at the level of the anterior communicating artery, 2) and 3) (arrow) at the right middle cerebral artery (MCA) bifurcation, 4) at the left MCA bifurcation. The largest aneurysm at the right MCA bifurcation shows a “tit” (arrowhead), signaling that this aneurysm was probably the one responsible for the subarachnoid hemorrhage (already suspected due to the distribution of the subarachnoid blood). The reformations also precisely demonstrate that no arterial branch arises from the aneurismal sac and display the orientation of the

aneurysm and its location with respect to the parent vessel and the bone. The patient did not undergo a conventional angiogram; she went directly to the operating room for clipping of the ruptured right MCA aneurysm.

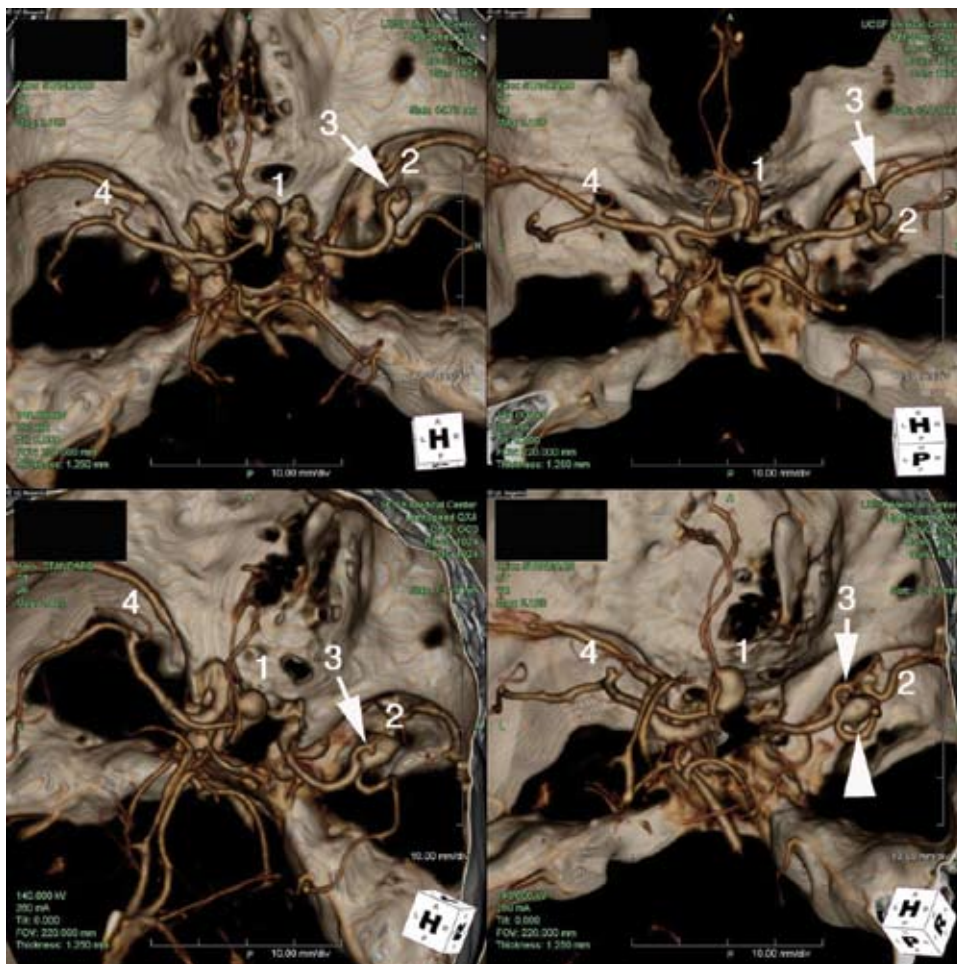
### Discussion:

CT-angiography is fast becoming a standard method for evaluation of a patient with subarachnoid hemorrhage. Using the Aquarius Workstation 3D post processing algorithms, aneurysms can be detected with a high degree of sensitivity and specificity. 3D reconstructions provide the neurosurgeon with unique spatial information regarding the configuration of the aneurysm and its relationship to the adjacent vessels and bony elements. This technique helps in treatment planning as well as training neurosurgeons about the expected surgical anatomy.

Some have advocated CT-angiography as the sole imaging examination required before aneurysm therapy.

### References:

- Hoh BL, Cheung AC, Rabinov JD, Pryor JC, Carter BS, Ogilvy CS. Results of a prospective protocol of computed tomographic angiography in place of catheter angiography as the only diagnostic and pretreatment planning study for cerebral aneurysms by a combined neurovascular team. *Neurosurgery* 2004;54(6):1329-1340.
- Karamessini MT, Kagadis GC, Petsas T, Karnabatidis D, Konstantinou D, Sakellariopoulos GC, Nikiforidis GC, Siablis D. CT angiography with three-dimensional techniques for the early diagnosis of intracranial aneurysms. Comparison with intra-arterial DSA and the surgical findings. *Eur J Radiol* 2004;49(3):212-223.
- Kangasniemi M, Makela T, Koskinen S, Porras M, Poussa K, Hernesniemi J. Detection of intracranial aneurysms with two-dimensional and three-dimensional multislice helical computed tomographic angiography. *Neurosurgery*. 2004;54(2):336-340



### Case 3: CT of the Cervical Spine in a Severe Trauma Patient

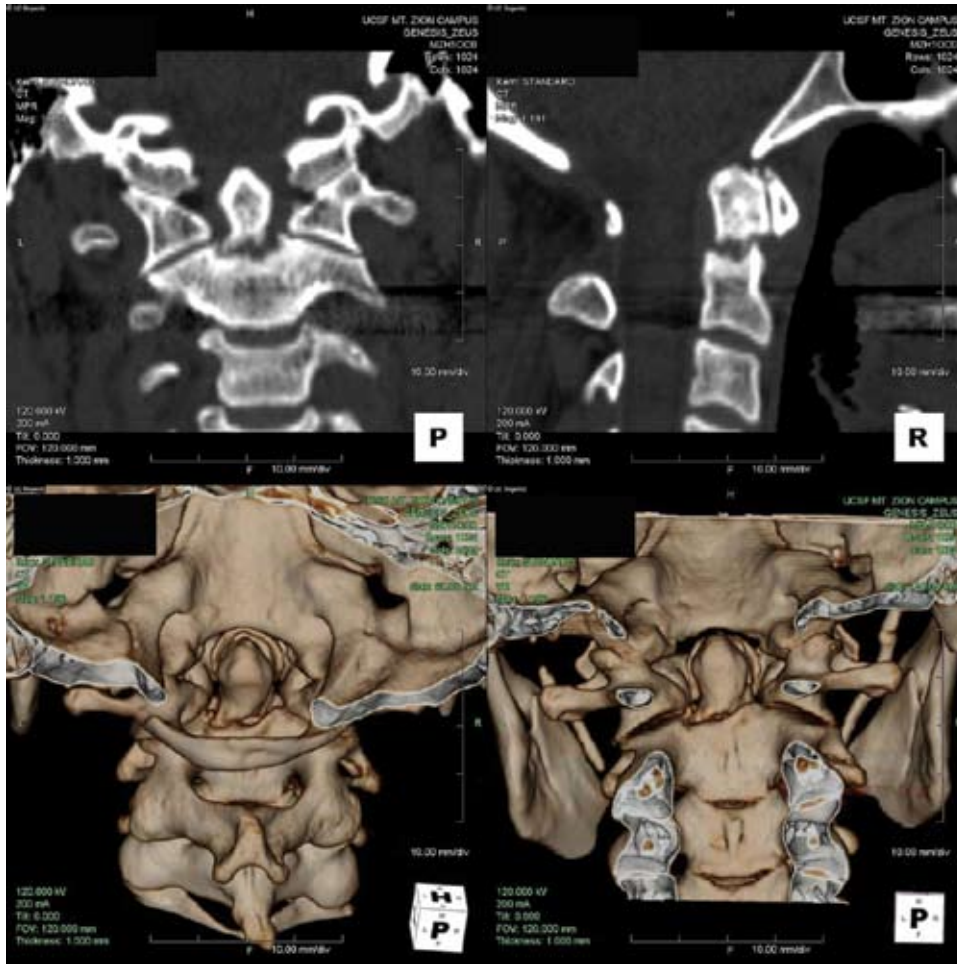
*Max Wintermark, M.D., William P. Dillon, M.D.*

#### History:

The patient is a male aged 31, involved in a severe motor vehicle accident. He was admitted with neck pain. He initially underwent plain films of the cervical spine, which were of poor quality because of his sling and motion artifact. He was transported to the CT room, where he underwent a CT of the brain, a CT of the neck, and a CT-aortogram of the chest, abdomen and pelvis.

#### Protocol Description:

Scan Information	Type of Scanner	Lightspeed 16
	Scan Region	Neck
	Scan Length	25 cm
	Scan Direction	Craniocaudal
	Detector Configuration	16 x 0.625
	Pitch	1.375:1
	Tube Voltage	120 kVp
	Tube Current	240 mA
	Rotation Time	0.5 sec
	Total Acquisition Time	12 sec
	Field of View	18 cm
Reconstruction Information	Reconstruction Algorithm	Bone
	Slice Thickness	1.25
	Reconstruction Interval	1
	Total Number of Images	250
Contrast Information	Contrast	No contrast
	Concentration	-
	Volume	-
	Injection Rate	-
	Timing Method	-



**Results:**

The 2D coronal and sagittal reformations and the 3D reformats obtained from the CT of the cervical spine demonstrate accurate an unstable type II fracture of the odontoid process of C2. The fractured dens is slightly tilted in the posterior, but does not compromise the cervical vertebral canal. The 3D reformations using Aquarius Workstation were particularly useful for surgical planning.

**Discussion:**

Given the potentially devastating consequences in an individual in whom a spine fracture is missed, and the potential medical legal consequences for the involved physicians, all trauma patients should be cleared for their cervical spine within minutes after the patient’s admission into the emergency room. From this standpoint, routine CT of the cervical spine has proven cost-effective in the management of acute

trauma patients with suspected cervical spine injury. 3D reconstructions, as demonstrated in the example above, are essential for the accurate depiction and proper treatment of cervical spine fractures.

**References:**

Blackmore CC, Mann FA, Wilson AJ. Helical CT in the primary trauma evaluation of the cervical spine: an evidence-based approach. *Skeletal Radiol* 2000;29:632-639

Li AE, Fishman EK. Cervical spine trauma: evaluation by multidetector CT and three-dimensional volume rendering. *Emerg Radiol.* 2003;10(1):34-39.

Kosling S, Dietrich K, Steinecke R, Kloppel R, Schulz HG. Diagnostic value of 3D CT surface reconstruction in spinal fractures. *Eur Radiol.* 1997;7(1):61-64.

## Case 4: Abdominal CT-arteriogram in a Patient with Renal Artery Stenosis

*Fergus Coakley, M.D.*

### History:

The patient is a male, aged 9. He had been diagnosed with hypertension 8 years after chemotherapy and resection for neuroblastoma. Surgery was complicated by inadvertent transection of the right renal artery requiring reimplantation, and by postoperative left renal artery thrombosis leading to complete atrophy of the left kidney.

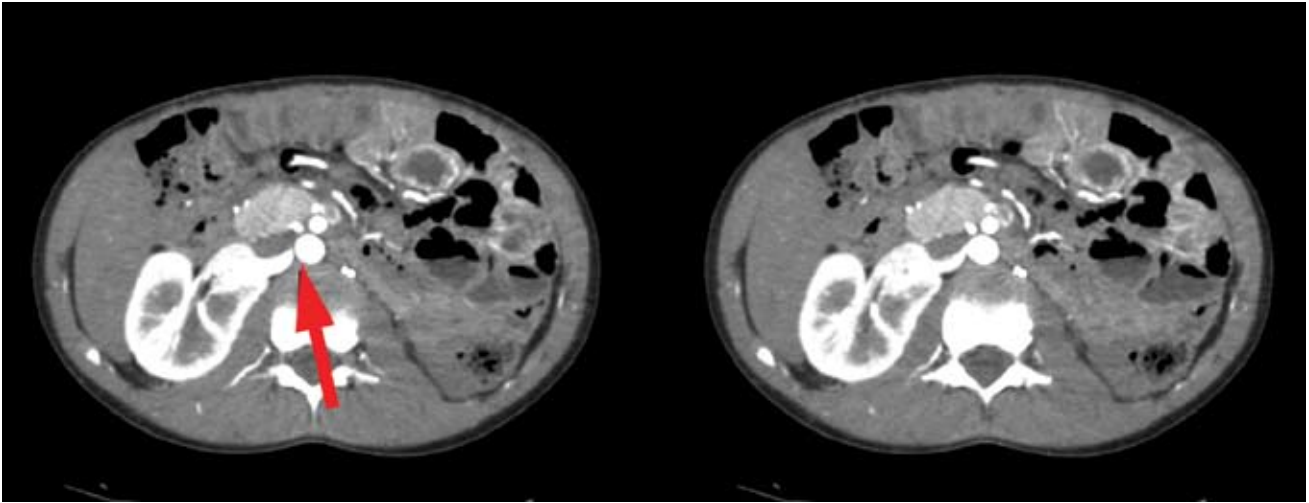
### Protocol Description:

Scan Information	Type of Scanner	Lightspeed 16
	Scan Region	Abdomen
	Scan Length	60 cm
	Scan Direction	Craniocaudal
	Detector Configuration	16 x 1.25
	Pitch	1.375:1
	Tube Voltage	120 kVp
	Tube Current	400 mA
	Rotation Time	0.8 sec
	Total Acquisition Time	15 sec
	Field of View	38 cm
Reconstruction Information	Reconstruction Algorithm	standard
	Slice Thickness	1.25
	Reconstruction Interval	1.00
	Total Number of Images	600
Contrast Information	Contrast	Omnipaque
	Concentration	300 mg/mL
	Volume	150 mL
	Injection Rate	4 mL/sec
	Timing Method	20 sec delay

### Results:

The axial images show a subtle narrowing at the origin of the right renal artery (arrows).

The left kidney is not visible. The 3D images show the marked right renal artery stenosis to much better effect, with a marked narrowing (arrows) evident just downstream to the right renal artery ostium.



### Discussion:

This case illustrates how 3D images can help display clinically important information in a way that is more easily appreciated. While the pathology is evident on the axial images, the arteriographic quality of the reformations allows rapid identification of the vascular abnormality. CT angiography is a robust noninvasive examination for the diagnosis of renal artery stenosis, with an accuracy of over 90% and a specificity of nearly 100% in the diagnosis of severe (over 50%) stenosis. Normal results from CT angiography virtually rule out renal artery stenosis.

### References:

- Urban BA, Ratner LE, Fishman EK. Three-dimensional volume-rendered CT angiography of the renal arteries and veins: normal anatomy, variants, and clinical applications. *Radiographics*. 2001;21:373-386.
- Johnson PT, Halpern EJ, Kuszyk BS, et al. Renal artery stenosis: CT angiography-comparison of real-time volume rendering and maximum intensity projection algorithms. *Radiology* 1999;211:337-343.
- Qanadli SD, Mesurolle B, Coggia M, et al. Abdominal aortic aneurysm: pretherapy assessment with dual-slice helical CT angiography. *AJR Am J Roentgenol* 2000; 174:181-187.



## Case 5: Abdominal CT-arteriogram in a Patient with Pancreatic Cancer

*Fergus Coakley, M.D.*

### History:

The patient is a male, aged 62, with locally advanced and metastatic pancreatic cancer.

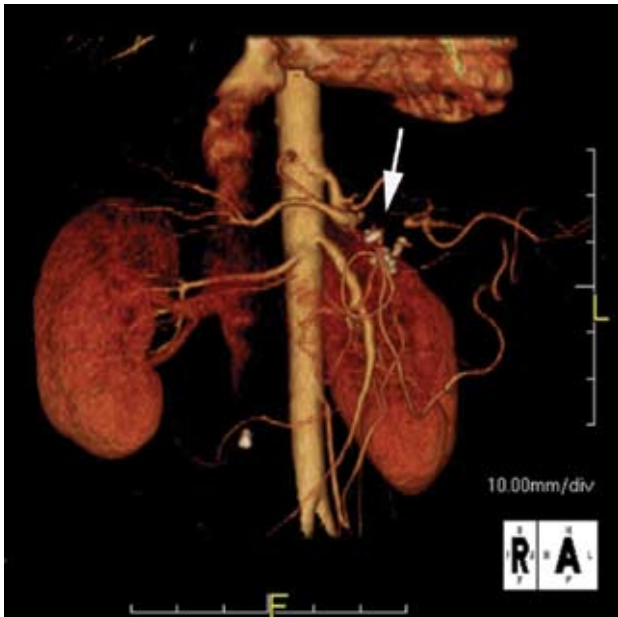
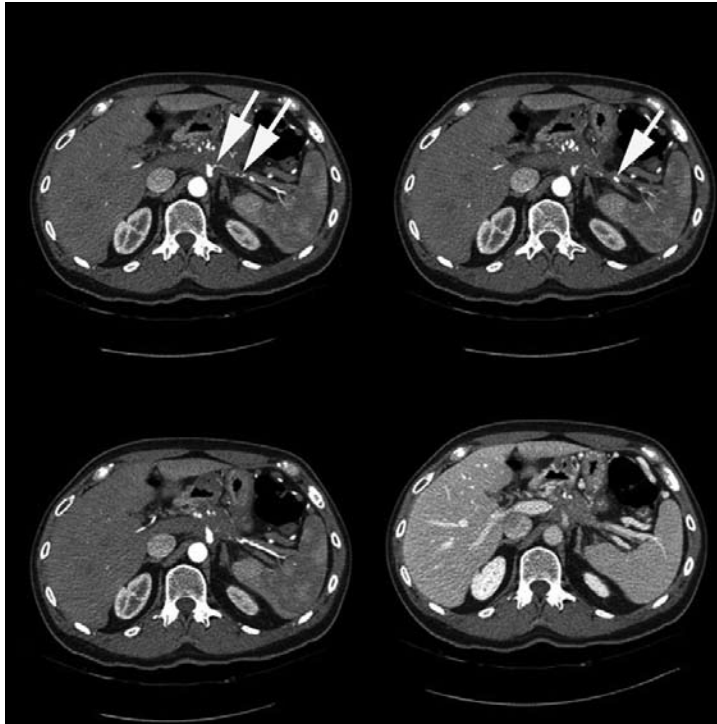
### Protocol Description:

Scan Information	Type of Scanner	Lightspeed 16
	Scan Region	Abdomen
	Scan Length	60 cm
	Scan Direction	Craniocaudal
	Detector Configuration	16 x 1.25
	Pitch	1.375:1
	Tube Voltage	120 kVp
	Tube Current	400 mA
	Rotation Time	0.8 sec
	Total Acquisition Time	15 sec
	Field of View	38 cm
Reconstruction Information	Reconstruction Algorithm	standard
	Slice Thickness	1.25
	Reconstruction Interval	1.00
	Total Number of Images	600
Contrast Information	Contrast	Omnipaque
	Concentration	300 mg/mL
	Volume	150 mL
	Injection Rate	4 mL/sec
	Timing Method	20 sec delay

### Results:

The axial images demonstrate a hypodense mass encasing the splenic artery just downstream from its origin off the celiac artery. The artery is critically stenosed (arrows) but remains patent.

The stenosed portion of the splenic artery (arrow) is barely visible on the 3D image, and could be mistaken for a complete occlusion.



**Discussion:**

While 3D imaging is of great value in presenting complex volumetric data in a way that highlights the structures of interest (such as vessels) and is of proven utility in the evaluation of vascular involvement in pancreatic cancer, care must be taken in interpreting these reformatting images. Potential artifacts include making critical stenoses appear like complete occlusions. It is important to correlate 3D findings with the corresponding 2D images in order to avoid such pitfalls.

**References:**

Takeshita K, Furui S, Takada K. Multidetector row helical CT of the pancreas: value of three-dimensional images, two-dimensional reformations, and contrast-enhanced multiphase imaging. *J Hepatobiliary Pancreat Surg* 2002; 9: 576-582.

**Case 6: Anomalous Drainage of the Right Posterior Segmental Bile Duct into the Left Hepatic Bile Duct in a Potential Partial Liver Donor**

*Richard S. Breiman, M.D.*

**History:**

The patient is a female, aged 37, and is a potential partial liver donor.

**Protocol Description:**

Scan Information	Type of Scanner	Lightspeed 16
	Scan Region	Liver
	Scan Length	20 cm
	Scan Direction	Craniocaudal
	Detector Configuration	16 x 1.25
	Pitch	1.375:1
	Tube Voltage	120 kVp
	Tube Current	400 mA
	Rotation Time	0.8 sec
	Total Acquisition Time	15 sec
	Field of View	38 cm
Reconstruction Information	Reconstruction Algorithm	standard
	Slice Thickness	1.25
	Reconstruction Interval	1.00
	Total Number of Images	600
Contrast Information	Contrast	Cholografin meglumine
	Concentration	10.3%
	Volume	100 mL
	Injection Rate	30 min infusion
	Timing Method	15 min delay



**Results:**

Axial scans demonstrate normal caliber intra and extra-hepatic bile ducts. Anomalous drainage of right ducts is not appreciated in this projection.

Maximum intensity projection (MIP) images and volume rendered (VR) images demonstrate anomalous drainage of the right posterior segment hepatic bile duct to the left hepatic bile duct.

## Discussion:

As part of the pre-operative evaluation of a potential partial liver donor, the course and patency of hepatic arteries, hepatic veins, portal veins and bile ducts are assessed. An unsuspected anomalous course of these structures may lead to post-operative complications in both the donor and the recipient of a partial liver transplant. A potential partial liver donor with anomalous drainage of a branch of the right hepatic bile duct to the left hepatic bile duct is considered a higher risk donor than a potential donor with conventional biliary drainage. Although a donor candidate with anomalous biliary drainage may be selected for donation in some centers, the transplant surgeon needs to be prepared to create an anastomosis of the small caliber right ductal branch to the common bile duct of the recipient. Such an anastomosis prolongs surgery and is associated with an increased incidence of post-transplant cholangitis. MRCP has on occasion lacked the necessary spatial resolution to detect anomalous drainage of the normal caliber bile ducts of potential partial liver donors. CT cholangiography, utilizing thin slice MDCT of bile ducts opacified by contrast excreted by the liver into the biliary system, is better able to assess small caliber bile ducts than



MRCP. Multiplanar and 3D image processing enhances appreciation of the subtle anomalous course of bile ducts.

In this case, the posterior segmental right hepatic bile duct terminates in the left hepatic duct near its junction with the right hepatic duct. Due to the close proximity of these ducts, the anomaly was not recognized on the source axial CT scans and was only appreciated on the maximum intensity projection and volume rendered images.

## References:

Yeh BM, Breiman RS, Taouli B, Qayyum A, Roberts JP, Coakley FV. Biliary tract depiction in potential liver donors: Comparison of conventional MR, Mangafodipir Trisodium-enhanced excretory MR, and multi-detector row CT. *Radiology*, 230: 645-651, 2004.

Lee VS, Morgan GR, Teperman LW, et al. MR imaging as the sole preoperative imaging modality for right hepatectomy: a prospective study of living adult-to-adult liver donor candidates. *AJR Am J Roentgenol* 2001; 176:1475-1482.

Schroeder T, Nadalin S, Strattaus J, Debatin JF, Malago M, Ruehm SG. Potential living liver donors: evaluation with an all-in-one protocol with multi-detector row CT. *Radiology* 2002; 224:586-591.